HEAT TRANSFER DURING MELTING OF A SUBSTANCE IN A CLOSED VOLUME WITH HEATING FROM BELOW

V. V. Galaktionov and A. P. Ezerskii

UDC 536.2.01

The authors have conducted a numerical experiment on which they have based an engineering technique for determining the heat transfer characteristics.

Among the possible uses of fusible substances for heat energy storage there is great interest in their use in solar energy storage systems. In the last decade the number of papers addressing this topic has increased appreciably. In experimental studies, conducted with various substances and geometrical systems [1-4], the main attention has been paid to the role of free convection, whose influence on the melting process has precluded the use of analytical and approximate solutions based on models of "pure" heat conduction.

Many numerical investigations have also addressed this topic. For example, [5, 6] used simplified transfer equations to analyze free convection in melting, respectively, around a vertical cylinder and near a vertical wall. References [7-9] gave results of melting outside and inside a horizontal cylinder and near a vertical wall, mapping the region into a rectangle.

The present paper examines melting of a substance located in a closed volume, with heating from below. The following assumptions are made: 1) the Boussinesq approximation is used for the liquid phase; 2) the phase densities are the same; 3) the flow is laminar and two-dimensional. In reality the flow will be two-dimensional in the case when the thickness of the closed volume is appreciably less than its length and height.

To overcome the difficulties associated with a time-dependent melt region, the latter is transformed into a rectangle with fixed boundaries [10]. We write the dimensionless equations describing the process in the transformed region in the following generalized form (Table 1):

$$\varepsilon \operatorname{Ste} \Phi_\tau + u\Phi_\xi + v\Phi_\eta = \Gamma \Delta \Phi + S. \tag{1}$$

In integrating this equation we use the conservative form for representing the convective and diffusion terms:

$$u\Phi_\xi + v\Phi_\eta = (u\Phi)_\xi + (v\Phi)_\eta - \Phi(u_\xi + v_\eta), \tag{2}$$

$$\Delta\Phi = (\alpha\Phi_\xi + \beta\Phi_\eta)_\xi + (\beta\Phi_\xi + \gamma\Phi_\eta)_\eta. \tag{3}$$

The transformed coordinates and the position of the phase boundary have the form (Fig. 1):

$$\xi = \frac{x - x_1}{x_2 - x_1}, \quad \eta = \frac{y - y_1}{y_2 - y_1}, \quad s = \frac{x_2 - x_1}{y_2 - y_1}. \tag{4}$$

It is assumed at the initial time ($\tau = 0$) that the system temperature is uniform ($\theta = 0$), and then the temperature of the heating surface is increased in a step manner to some steady

TABLE 1. Values of Generalized Parameters for Eq. (1)

Φ	ε	Γ	S
ω	1	Pr	$-\operatorname{Ra}\operatorname{Pr}(\theta_\xi \xi_y + \theta_\eta \eta_y) h$
ψ	0	1	$-\omega$
θ	1	1	0

Moscow Power Institute. Translated from Inzhenerno-Fizicheskii Zhurnal, Vol. 49, No. 5, pp. 756-763, November, 1985. Original article submitted October 1, 1984.

 0022-0841/85/4905-1286$09.50

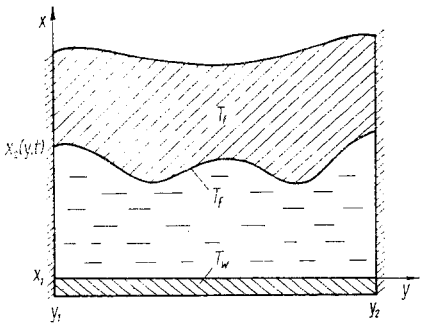

Fig. 1

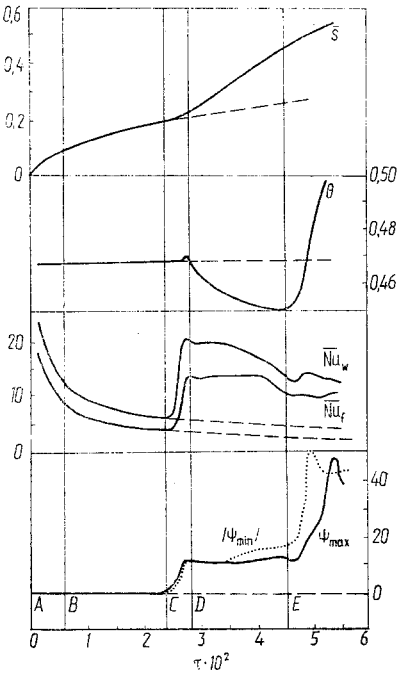

Fig. 2

Fig. 1. Schematic of the model problem.

Fig. 2. Behavior of the integral characteristics of the process with time: $Ra = 2 \cdot 10^6$, $Ste = 1$. The broken lines correspond to the model with pure heat conduction.

value ($\theta = 1$). Since the computing mesh covering the liquid phase cannot be infinitely fine, the calculation begins with the condition of practically no convective motion in the melt:

$$s_0 < (Ra_h^*/Ra)^{1/3}, \tag{5}$$

and here the interface surface is parallel to the heating surface. The value of the internal Rayleigh number Ra^*_h corresponding to the appearance of hydrodynamic instability was defined in [11], and is analogous to the critical Rayleigh number in the classical Benard problem.

Knowing the initial thickness of the melt s_0 and using the exact solution of [12], we can determine the dimensionless time corresponding so s_0 and the temperature distribution:

$$\tau_0 = s_0^2 \, Ste/4\sigma^2, \quad \theta_0 = 1 - \operatorname{erf}(\xi\sigma)/\operatorname{erf}(\sigma), \tag{6}$$

where σ is found from the equation

$$\sigma/Ste = \exp(-\sigma^2)/\sqrt{\pi}\operatorname{erf}(\sigma). \tag{7}$$

Here, to single out the processes occurring in the liquid phase, it is assumed that the solid phase is at the melting temperature, i.e., that the heat transferred through the melt is completely stored at the interface boundary. Reference [13] has estimated how this assumption affects the heat and mass transfer characteristics. Following this simplification, the energy balance at the phase interface boundary can be written as follows:

$$-s\alpha\theta_\xi|_{\xi=1} = s_\tau. \tag{8}$$

The remaining boundary conditions have the form:

$$\left.\begin{array}{l} \xi = 0, \ \theta = 1, \\ \xi = 1, \ \theta = 0, \end{array}\right\} \quad \psi = 0, \ \omega = \alpha\Phi_{\xi\xi}, \qquad \left.\begin{array}{l} \\ \\ \eta = 0, \ 1, \ \theta_\eta = 0, \ \psi = 0, \ \omega = \gamma\Phi_{\eta\eta}. \end{array}\right\} \tag{9}$$

In constructing the finite-difference approximation of Eq. (1) we used a control volume method, along with an exponential scheme for calculating the coefficients [14]. The result-

ing finite-difference analog was solved using the SOR method. The variables were calculated in the following order: 1) construction of the $\xi-\eta$ mesh; 2) computation of the initial conditions of Eqs. (5)-(7); 3) calculation of the transformation coefficients α, β, γ, J, P, Q on the basis of Eqs. (4) and (8); 4) alternate calculation of the coefficients and solution of the finite difference analog for ψ, ω, θ; 5) calculation of the boundary conditions of Eq. (9); 6) repeat of steps 3-5 to achieve the required step size.

The basic calculations were performed on a uniform 11 × 41 mesh, and a check calculation was made on a 17 × 48 mesh. The error in all the variables did not exceed $|1 - \Phi^{(k)}_{i,j}/\Phi^{(k+1)}_{i,j}| < 10^{-3}$. The time step was chosen from the stability conditions and varied during the calculation as a function of the number of iterations over the variable from 10^{-5} to $1.5 \cdot 10^{-4}$.

It can be seen from analysis of Table 1 that to characterize the process fully one must assign the Ra, Ste, and Pr numbers. Since it is known from previously published studies [5, 6] that in the region $Pr \geq 1$ for the type of problem examined the results are practically independent on the last of these, in this work we conducted two series of calculations – with fixed Ste = 0.5 and Pr = 1, and with fixed $Ra = 5 \cdot 10^5$ and Pr = 1. The ranges of variation were chosen from the operating conditions of the heat energy storage systems: Ste = 0.063-1.000, $Ra = 5 \cdot 10^5$-10^7.

It should be noted that all the calculations were begun with a nonzero distribution of ψ and ω, corresponding to a very small initial slope of the cavity (10^{-4}). In actuality, this kind of perturbation is inevitable because nonuniformities of some kind are present in the liquid phase.

The integral characteristics describing the dynamic structure of the melt as a whole are shown in Fig. 2. To better understand the processes occurring in the melt, we used visualization during the numerical experiment. Figure 3 shows instantaneous pictures of the flow and the heat transfer, obtained with the aid of a special program, including linear interpolation of intermediate values of the function. On the basis of these data (in a fuller volume) we describe and analyze the process below.

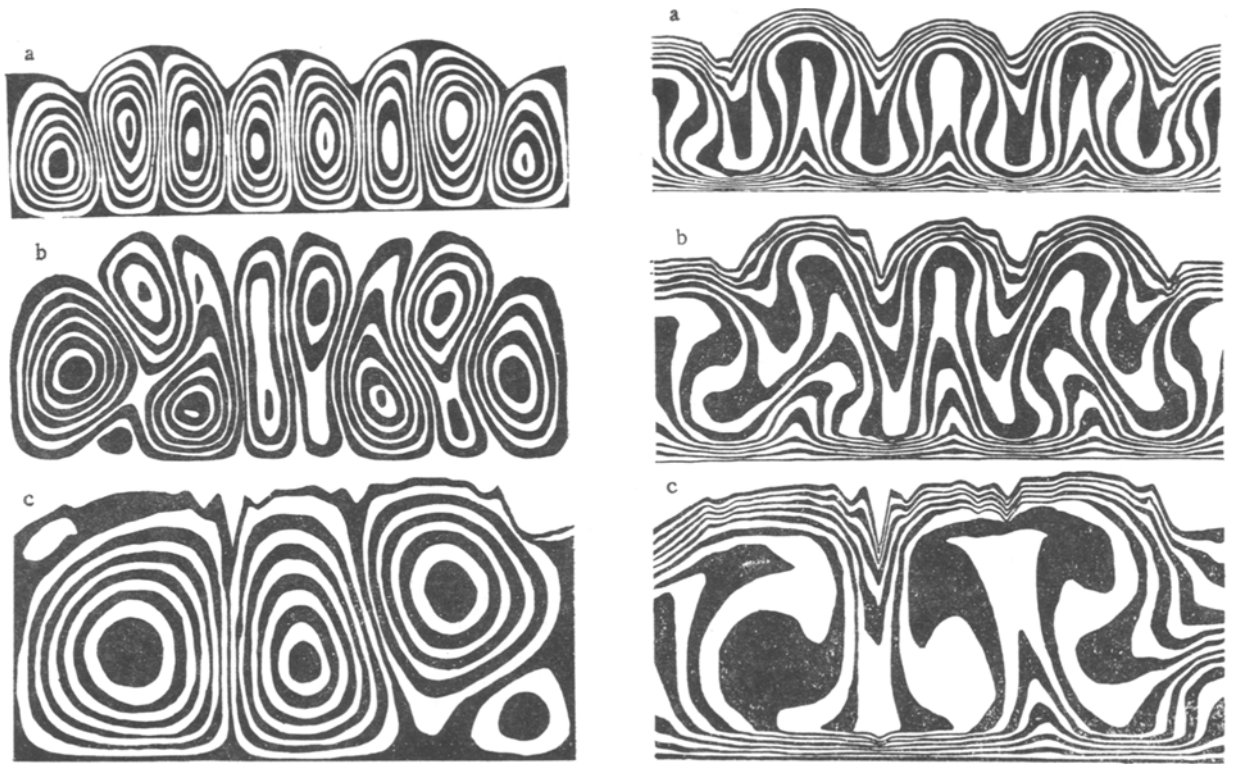

Fig. 3. Instantaneous pictures of the flow (on the left), and heat transfer in the melt (on the right): $Ra = 2 \cdot 10^6$, Ste = 1, τ = 0.035 (a), 0.045 (b), 0.055 (c).

TABLE 2. Characteristics of the Melting Process for the Heat Conduction Regime

Ste	$\varkappa$	B_w	B_f
1,000	0,124	1,120	0,770
0,500	0,132	1,075	0,868
0,250	0,136	1,038	0,938
0,125	0,139	1,023	0,962
0,063	0,140	1,012	0,980
$\to 0$	$\to \sqrt{2}$	$\to 1,000$	

TABLE 3. Characteristics of the Melting Process for the Pseudostationary Convection Regime

Ste	Ra_c^*	C_w	C_f
1,000	14000±12%	0,153	0,115
0,500	9000±8%	0,148	0,119
0,250	6000±5%	0,135	0,121
0,125	4300±3%	0,128	0,122
0,063	3500±3%	0,125	0,122
$\to 0$	$\to 1708$ (?)	$\to 0,123$	

The start of the calculation is accompanied by a redistribution of the initial perturbations, which are gradually damped. In the vicinity of the value $Ra^*_h \approx 1700$ [11], we observe a "neutral" equilibrium ($\psi_{max} \approx -\psi_{min} \approx 10^{-4}$). A subsequent increase of the melt thickness leads to a gradual increase of the convection intensity, but the heat transfer mechanism remains conduction as beofre (see Fig. 2, section BC). One can call this period of melting the thermal inertia period, whose duration increases with increase of the Ste number. This period is characterized by the presence of alternating weak vortex cells of opposite sign, their number depending on the Ra number and on the dimensionless melt thickness. It should be noted that in individual cases we observed an odd number of vortices, but because of its instability this kind of structure quickly underwent transition to an even number of cells.

The thermal inertia period is ended by the onset of a thermal instability. This short-duration transition period is associated with a sharp increase of intensity of the vortices and of the heat transfer (section CD).

The state that sets in subsequently is characterized by quasistationary vortex cells which transmit a practically constant amount of heat through the melt. An almost isothermal core and large temperature gradients form near the heat transfer surfaces (Fig. 3a). Because of the increased heat removal surface more energy is absorbed on it than in the case when this surface remains planar. Consequently, there is some increase of the bulk temperature of the melt (see Fig. 2, section DE).

The most interesting feature of this melting period is the fact that the average speed of motion of the melt front, equal to Nuf, is constant, while the average coordinate of the interface boundary (or the melt mass) depends linearly on time.

Further increase of the melt region leads to the situation where the strongly deformed vortices can no longer retain their shape. This results in the start of a general redistribution of the flow, accompanied by relative displacement of the vortices, and expulsion of some due to increased size of neighboring vortices (Fig. 3b, c). The rather high degree of symmetry observed prior to this breaks down, the flow becomes unstable, and there may be low-frequency oscillations of the heat transfer characteristics. The redistribution of the heat flux leads to a smoothing of the interface surface. In spite of the fact that the intensity of vortex motion increases in this melting period, nevertheless the heat transfer decreases. This latter circumstance is apparently linked with an increase of the size of the vortex cell, which now itself stores some part of the heat energy transferred through the melt. This is evidenced by an increase of the melt bulk temperature.

Because of the excessive length of the calculations, this period was reached only for one set of the governing parameters. The first two basic melting periods are of interest for practical purposes, as a rule.

For the melting period, characterized by heat conduction, the Nusselt number on both of the heat transfer surfaces and the position of the phase interface surface can be determined by using the exact solution:

$$\mathrm{Nu} = B/s, \quad s = \varkappa\sqrt{\tau}, \quad \varkappa = 2\sigma/\sqrt{\mathrm{Ste}}, \tag{10}$$

where the quantities κ, B_w, and B_f, which depend only on the Ste number, are given in Table 2.

For the subsequent pseudostationary convection regime it was found, from analysis of the parametric dependence on the Ra number, that the average values of Nu number on these surfaces are given by the relation

$$\overline{\mathrm{Nu}} = C\mathrm{Ra}^{1/3}. \tag{11}$$

We notice that the characteristic length contained on the left and right sides of Eq. (11) is contracted. This means that the heat transfer coefficient is not determined by the length of the closed volume.

In Eq. (11) the local Nu numbers were calculated on both boundaries from the relation

$$\mathrm{Nu} = -s\alpha\theta_{\xi}. \tag{12}$$

For the phase interface this kind of determination is arbitrary, but its use is convenient, since in that case the Nu number is equal to the local velocity of motion of the interface, as follows from Eq. (8). Averaging Eq. (8) and taking account of Eq. (12), we obtain the dependence

$$\overline{\mathrm{Nu}}_f = d\bar{s}/d\tau, \tag{13}$$

and integration of this in the time interval of interest to us gives

$$\bar{s} = C_f\mathrm{Ra}^{1/3}(\tau - \tau_c) + s_c, \tag{14}$$

i.e., the average melt thickness, as noted above, depends linearly on time for the melting period considered. This behavior corresponds to the experimental results on melting of paraffin in an analogous geometry [1].

We shall determine the unknown quantities τ_c and s_c appearing in Eq. (14):

$$\tau_c = (s_c/\varkappa)^2, \quad s_c = (\mathrm{Ra}_c^*/\mathrm{Ra})^{1/3}. \tag{15}$$

Thus, to evaluate the integral characteristics of the melting process in a closed cavity with isothermal heating from below, the following method is proposed: 1) determine the Ra and Ste numbers; 2) determine from Table 2 and Eq. (10) the characteristics for the heat conduction regime; 3) determines C_w, C_f, and the internal critical Rayleigh number Ra^*_c from Table 3; 4) calculate critical values of time and melt thickness from Eq. (15); and, 5) calculate the $\overline{\mathrm{Nu}}$ number and the mass of melted substance on the basis of Eqs. (11) and (14).

In conclusion, we note some special features of the results. First, the origin of the thermal instability is displaced relative to the hydrodynamic origin, and the Ra^*_c number depends more strongly on the Ste number than does Ra^*_h value found from linear stability theory [11]. Secondly, the quantities C_w and C_f are also determined by the Ste number, although they depend only weakly on the latter in the region $\mathrm{Ste} \to 0$.

NOTATION

Φ, generalized variable; x, y, physical coordinates; t, time; ξ, η, transformed coordinates; S, dimensionless coordinate of the phase interface; $\tau = \mathrm{FoSte}$, dimensionless time; ψ, ω, dimensionless stream function and vorticity; $\theta = (T - T_f)/(T_w - T_f)$, dimensionless temperature; $u = \varepsilon(\mathrm{Ste}\,\xi_\tau - J\psi_\eta) + \Gamma P$, $v = \varepsilon(\mathrm{Ste}\,\eta_\tau + J\psi_\xi) + \Gamma Q$, transformed velocities; $\alpha = (\xi_x^2 + \xi_y^2)h^2$, $\beta = (\xi_x\eta_x + \xi_y\eta_y)h^2$, $\gamma = (\eta_x^2 + \eta_y^2)h^2$, $J = (\xi_x\eta_y - \xi_y\eta_x)h^2$, $P = \alpha\xi + \beta\eta - (\xi_{xx} + \xi_{yy})h^2$, $Q = \beta\xi + \gamma\eta - (\eta_{xx} + \eta_{yy})h^2$, transformation coefficients; $\mathrm{Fo} = at/h^2$, $\mathrm{Ste} = c(T_w - T_f)/L$, $\mathrm{Ra} = g\hat{\beta}(T_w - T_f)h^3/\nu a$, $\mathrm{Pr} = \nu/a$, $\mathrm{Nu} = \hat{\alpha}h/\lambda$, Fourier, Stefan, Rayleigh, Prandtl, and Nusselt numbers; $\mathrm{Ra}^* = g\hat{\beta}(T_w - T_f)(x_2 - x_1)^3/\nu a = \mathrm{Ra}\bar{s}^3$, internal Rayleigh number; $h = y_2 - y_1$, characteristic length; a, thermal diffusivity; c, specific heat; T, temperature; L, specific heat of fusion; ν, kinematic viscosity; g, acceleration due to gravity; $\hat{\beta}$, coefficient of thermal expansion; $\hat{\alpha}$, heat removal coefficient; λ, thermal conductivity. Subscripts: x, y, t, ξ, η, τ, differentiation; 0, initial time value; h, hydrodynamic; c, critical; w, heating wall; f, phase interface surface. Averaging: $\bar{\Phi} = \int_0^1 \Phi d\eta$, $\bar{\bar{\Phi}} = \int_0^1\int_0^1 \Phi d\xi d\eta$.

LITERATURE CITED

1. N. W. Hale and J. and R. Viskanta, "Solid-liquid phase change heat transfer and interface motion in materials cooled or heated from above or below," Int. J. Heat Mass Transfer, 23, 283-292 (1980).
2. A. G. Bathelt and R.Viskanta, "Heat transfer at the solid-liquid interface during melting from a horizontal cylinder," Int. J. Heat Mass Transfer, 23, 1499-1503 (1980).

3. P. D. Van Buren and R. Viskanta, "Interferometric measurement of heat transfer during melting from a vertical surface," Int. J. Heat Mass Transfer, 23, 568-571 (1980).
4. Sparrow and Broadbent, "The melting process in a vertical tube, allowing expansion of the medium with phase changes," Teploperedacha, No. 2, 85-92 (1982).
5. Sparrow, Patankar, and Ramal'yani, "Analysis of melting with natural convection in the melt," Teploperedacha, No. 4, 15-22 (1977).
6. V. V.Galaktionov and A. P. Ezerskii, "Analysis of the melting process, accounting for free convection," Dep. VINITI, No. 5906-82.
7. H. Rieger, U. Projahn, and H. Beer, "Analysis of the heat transport mechanism during melting around a horizontal circular cylinder," Int. J. Heat Mass Transfer, 25, 137-147 (1982).
8. C.-J. Ho and R. Viskanta, "Heat transfer during melting in a horizontal tube," Int. J. Heat Mass Transfer, 27, 705-716 (1984).
9. C.-J. Ho and R. Viskanta, "Heat transfer during melting from an isothermal vertical wall," J. Heat Transfer, 106, 12-19 (1984).
10. A. P. Ezerskii, "Method of solving the problem of convection and heat transfer in regions whose boundary shape varies with time," Inzh.-Fiz. Zh., 48, Issue No. 5, 765-771 (1985).
11. Sparrow, Lee, and Shamsudar, "Convective instability in a melting layer heated from below," Teploperedacha, No. 1, 94-102 (1976).
12. A. V. Lykov, Theory of Heat Conduction [in Russian], Vysshaya Shkola, Moscow (1967).
13. Sparrow, Ramad'yani, and Patankar, "The influence of supercooling of a solid medium on its melting in a cylindrical layer," Teploperedacha, Issue No. 3, 10-17 (1978).
14. S. Patankar, Numerical Methods of Solving Problems of Heat Transfer and Dynamics of a Liquid [in Russian], Énergoizdat, Moscow (1984).

DETERMINATION OF THE HEAT FLUX ON THE SURFACE OF COMPOSITE MATERIALS UPON INTERACTION WITH HIGH-ENTHALPY GAS STREAM

V. E. Abaltusov, S. F. Bachurina, G. Ya. Mamontov, G. A. Surkov, and A. S. Yakimov

UDC 536.245.022

The article deals with the determination of heat fluxes on the surfaces of composite materials upon interaction with a gas stream of high enthalpy.

For the calculation of processes of heat and mass exchange occurring upon interaction of composite heat insulating materials with a gas stream, and for the evaluation of the efficiency of the material it is indispensable to know the boundary conditions on the surface, in particular the specific heat flux [1, 2]. It is difficult, and in many cases altogether impossible, to measure it directly because of the physicochemical transformations occurring on the surface of and inside the material. The problem of finding specific heat fluxes usually reduces to the solution of the inverse problem for the equation of nonsteady heat conduction on the basis of experimentally measured temperature fields in the material.

The present work involves the determination of the heat fluxes on the interface of the media by different methods on the basis of the experimental data in measurements of the surface temperature and of the temperature field within the bulk of the specimen of composite material.

The experiments were carried out in jets of air plasma of an electric-arc plasmatron ÉDP-104A and a vortex plasmochemical reactor (PCR) with the following parameters of the stream: enthalpy of the gas H_0 = 2-10 MJ/kg; Reynolds numbers Re = $(0.5\text{-}5)\cdot 10^3$, Ma $\leq$ 0.3. The gas temperature in the jet was determined by the method of relative intensities with a spectro-

A. V. Lykov Institute of Heat and Mass Transfer, Academy of Sciences of the Belorussian SSR, Minsk. Translated from Inzhenerno-Fizicheskii Zhurnal, Vol. 49, No. 5, pp. 763-769, November, 1985. Original article submitted September 20, 1984.

0022-0841/85/4905-1291$09.50